Journal of Applied Electrochemistry **31**: 469–474, 2001.

Electrooxidation of cyanide on cobalt oxide anodes

A. STAVART[1]* and A. VAN LIERDE[2]
[1]*Meura Technologies/Ateliers de Monsville, Voie Minckelers 1, 1348 Louvain-la-Neuve, Belgium*
[2]*Université Catholique de Louvain (UCL), Département des Matériaux et des Procédés, Place S^te Barbe, 2–2° étage, 1348 Louvain-la-Neuve, Belgium*
*(*author for correspondence)*

Received 21 May 2000; accepted in revised form 24 October 2000

Key words: anodic oxidation, cyanide oxidation, electrooxidation, oxide electrode, wastewater treatment

Abstract

Oxidation of cyanide ions at a Ti/Co_3O_4 electrode in aqueous base solution has been investigated. The cyclic voltammetric curve for the oxidation of cyanide at Ti/Co_3O_4 shows a well formed wave prior to oxygen evolution at a potential where the spinel surface itself undergoes oxidation. Using a flow cell it is confirmed that the conversion of cyanide (CN^-) to cyanate (CNO^-) can be achieved galvanostatically with a reasonable current efficiency. As an example, at a current density of 100 A m^{-2}, CN^- concentration can be lowered from 10 to 0.2 mM with an electric energy consumption of about 18 kWh kg^{-1} of CN^- oxidized and a global current efficiency of 28.5%. The oxide coating appears to be quite stable during repeated electrolyses.

1. Introduction

Cyanide is a strong ligand able to complex many heavy metals. As a consequence, cyanides are widely employed in minerals extraction, metal finishing, electrodeposition and in some chemical syntheses. However, they constitute one of the most toxic and lethal species in industrial wastes. For this reason, based on aquatic toxicity tests, regulatory agencies have set point source emission limits of the order of 1 ppm. Consequently, in order to prevent surface and ground water contamination, procedures for the safe and proper treatment storage and handling of cyanide containing effluents are of primary concern.

Detoxification is generally achieved by the oxidation of cyanide to the 1000 times less toxic cyanate, mainly based on chemical methods such as alkaline chlorination, ozonation, hydrogen peroxide or air oxidation and sulphur-based technologies [1, 2]. Nevertheless, other techniques based on photolytic, photocatalytic, electrolytic and biological methods have been recently proposed [3–9].

Among these, the anodic oxidation of cyanide represents an attractive alternative since it obviates the need to store and handle large quantities of oxidant (such as chlorine or hydrogen peroxide) and prevents the formation of volatile toxic compounds. As classical electrolytic cells are designed to overcome mass transfer resistance between the bulk medium and the electrode surface, electrochemical oxidation of cyanide could be a faster treatment in a smaller and more compact unit than usual cyanide oxidation treatment plant.

The generally accepted mechanism for the first step of the cyanide electrooxidation is

$$CN^- + 2\,OH^- = CNO^- + H_2O + 2\,e^- \quad (1)$$

$$E = -0.143 - 0.0591\,pH + 0.00296 \times \log(CNO^-/CN^-)\ V \text{ vs SHE at } 25\ ^\circ C \quad (2)$$

Hartinger [1] described the electrochemical oxidation technique as the most environmentally friendly means for cyanide destruction. However, he pointed out that this two-electron transfer oxidation to form cyanate is a fairly slow reaction. For this reason, one of the major aspects to be considered is the nature of the working electrode which must be the most efficient and corrosion-resistant.

Platinum [10], steel [11] and lead [12] anodes have been used in many experiments for cyanide oxidation. Unfortunately, these electrodes exhibit poor current efficiency and, moreover, the latter two show poor resistance to corrosion. Graphite [13–16] is a more active anode but becomes slowly degraded during electrolysis. In recent years, more stable anodes have been successfully investigated. Recently, Perret et al. [17] have proposed an anode covered with a highly corrosion-resistant, thin diamond film. Galvanostatic experiments (360 A m^{-2}) show a current efficiency of 40% for concentrated cyanide solutions (1–0.5 M).

Electrodeposited PbO_2 has been demonstrated to be superior to graphite and stainless steel for CN^- oxidation. Poor current efficiency is observed, however, for

dilute solutions (< 0.2 M) [14, 18]. It was noted that the efficiency strongly depends on the surface properties of the PbO_2 coating. SnO_2 anodes increase the current efficiency by a factor of 2.5 when compared with Pt electrodes [19].

High oxygen overpotential and, more significantly, their capability to accumulate hydroxyl radicals on their surface are two reasons for the good behaviour of these stable electrodes. Wels and Johnson [20] suggest however, that a successful electrocatalysis of cyanide oxidation requires, not only sites for hydroxyl adsorption, but also available surfaces for adsorption of the reactant. Their investigation on the oxidation of cyanide on electrodeposited copper oxide in alkaline solutions has shown that the oxidation proceeds by oxygen transfer mediation facilitated by formation of Cu(III) sites in the CuO surface. These Cu(III) sites might function for adsorption of both the $OH^{\bullet}$ and the reactant. However, copper oxide was not stable in moderately concentrated cyanide solution (>1 mM) due to its dissolution as a copper tetracyanide complex $Cu(CN)_4^{2-}$.

Based on the high stability of $Fe(CN)_6^{3-}$ and $Fe(CN)_6^{4-}$, Feng and Johnson [21] have tested the activity of Fe(III) doped PbO_2 electrodes and discovered that oxidation of CN^- proceeds at a mass-transport controlled rate in alkaline media.

As cobalt cyanide complexes are also very stable [22], we report a study of the electrooxidation of cyanide ion in alkaline solution at a spinel-type Co_3O_4 film anode prepared by thermal decomposition of cobalt nitrate solution. Cobalt oxide is a readily available, low-cost product as compared with standard RuO_2 deposit. Since it also highly corrosion-resistant, it is presently being considered as a promising electrocatalyst for oxygen electrode in alkaline solution. Little work has been devoted, however, to its potential application in oxidation or reduction of species. Cox and Pletcher [23, 24] have used cobalt based spinel electrodes to oxidize alcohol and amine. Due to its higher efficiency, they conclude that the spinel coating may be used for many electrolyses without apparent loss of activity or physical–chemical damage.

2. Experimental details

2.1. *Electrode preparation*

Co_3O_4 electrodes were prepared by thermal decomposition of nitrate precursor deposited onto a titanium plate (Alfa). Ti plates were smoothly polished with emery paper, degreased in CH_2Cl_2, etched in concentrated nitric acid, rinsed with distilled water, and wiped with a filter paper. Immediately after pretreatment, a 0.5 M $Co(NO_3)_2 \cdot 6\ H_2O$ isopropanol solution was layered onto one face of the support. Then the support was dried at 60 °C to evaporate the solvent and heated in air at 300 °C for 10 min. Oxide layers were deposited by repeating this procedure 10 times to achieve full coverage of the metallic surface. Final annealing was done by keeping the sample for one hour at 300 °C to complete the thermal decomposition. The weight of the coating was typically 7.5 mg cm^{-2}.

The surface morphology of the oxide layers was examined using a Leica Stereoscan 260 scanning electron microscope equipped with an EDX system (EDAX). X-ray diffraction analyses were performed on a Siemens D500 diffractometer using CuK_α radiation.

This robust coating could be used for many experiments. X-ray (Figure 1(a)) diffraction spectra confirm that the layer has a Co_3O_4 spinel structure while SEM micrographs (Figure 1(b) and 1(c)) show that the coating has a continuous high surface area. It is also noticed that oxide aggregates appear here and there at the top of the surface. The unequal oxide film thickness is in the range of 1–10 μm, according to SEM analyses of the cross section (not shown).

2.2. *Cells and method*

Voltammetric and coulometric experiments were carried out in a compartimented cell. The Ti/Co_3O_4 working electrode was separated from a Pt gauze counter electrode by a cationic membrane (Nafion® 350, DuPont) and from the reference electrode (saturated calomel electrode, Schott-Geräte type B3410) by a Luggin capillary. Experiments were run on a computer-controlled EGG potentiostat (model 270A). Prior to use, the Ti/Co_3O_4 electrodes were preconditioned in the electrolyte solution at their open circuit potential for 5 min.

Galvanostatic experiments were carried out in a Microflow cell supplied by ElectroCell AB (Sweden). This undivided cell was equipped with a stainless steel cathode, the Co_3O_4 coated titanium anode and a turbulence promoter. The working electrode potential was controlled against a SCE connected to a Luggin capillary positioned close to the anode surface.

Plates of graphite (Alfa) and DSA–O_2 (ElectroCell AB) were also used as anodes for efficiency comparison. In each galvanostatic run, the electrode area was 10 cm^2 and the solution volume was 500 ml. A peristaltic pump circulated the electrolyte from a reservoir into the cell at a flow rate of 10 l h^{-1} corresponding to a linear flow velocity of about 2.5 cm s^{-1} inside the cell.

All solutions were prepared with deionized water and all chemicals were analytical grade. The CN^- concentration was determined by the standard titration method with a $AgNO_3$ solution and by a spectrophotometric method (spectrometer Perkin Elmer Lambda 20) according to ASTM norm D 2036–82. Cyanate ions were measured following the technique described by Henry and Boeglin [25]. After complete reduction of cyanate ions into ammonia ions, the ammonia concentration was determined by a spectrophotometric method using Nessler reagent. Cobalt ions concentration was determined by inductively coupled plasma spectrometer (ThermoOptek, Iris Advantage).

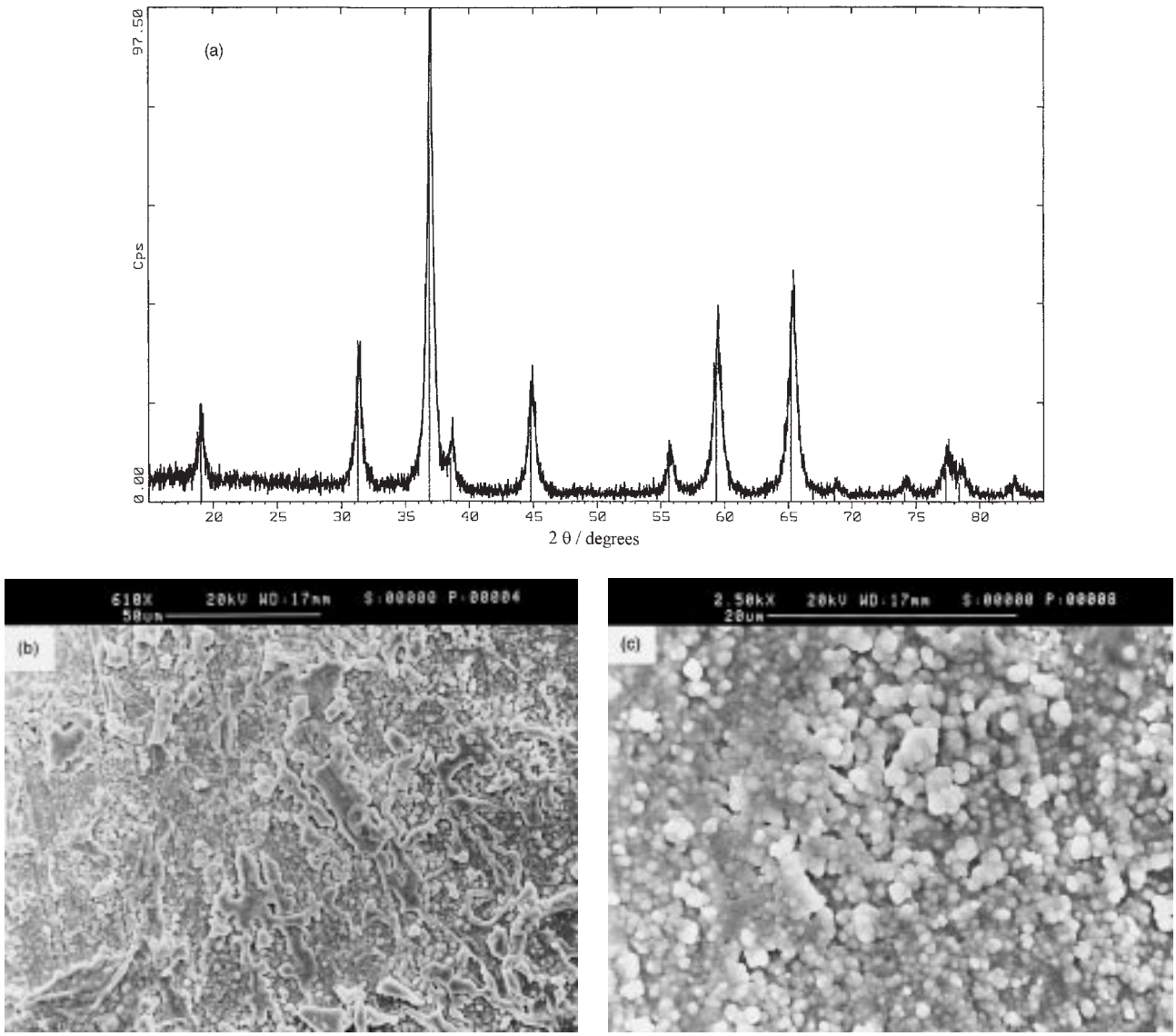

Fig. 1. X-ray diffractogram (a) and scanning electron micrographs (b) and (c) of Co_3O_4 prepared by thermal decomposition of $Co(NO_3)_2$ at 573 K on a Ti substrate.

3. Results and discussion

3.1. *Voltammetric experiments*

Cyclic voltammograms on Ti/Co_3O_4 electrodes were recorded at 25 °C in NaOH 0.1 M and Na_2SO_4 0.5 M for different sodium cyanide concentrations (0 M < NaCN < 0.1 M). The potential scan rate used was 20 mV s^{-1}. Figure 2 shows the characteristics of these voltammetric curves between open circuit potential and oxygen evolution. Garavaglia et al. [26] have shown that this open circuit potential is mainly determined by a surface equilibrium between Co^{2+}/Co^{3} in the oxide structure:

$$Co_3O_4 + 2\,H_2O = 3\,CoOOH + H^+ + e^- \qquad (3)$$

The rather large hysteresis between the anodic and cathodic current obtained respectively for the positive and negative scans could be explained by the double layer charging as the Co_3O_4 film was suspected to be very porous.

Without addition of cyanide ion, a single anodic peak at 780 mV vs SHE and its corresponding cathodic peak at 675 mV vs SHE are observed. According to Boggio et al. [27], these peaks correspond to the Co^{3+}/Co^{4+} transition on the oxide surface:

$$2\,CoOOH = CoO_2 + 2\,H^+ + 2\,e^- \qquad (4)$$

When the potential is taken positive to 850 mV vs SHE, a very large current is measured due to the initiation of oxygen evolution.

With cyanide ions present in solution (cyanide concentrations, respectively, 5.5 mM, 37.7 mM and 100 mM), the shapes of the voltammogram change significantly. The anodic current becomes larger and the reduction peak progressively disappears. That means that the Co^{4+} species present onto the electrode surface

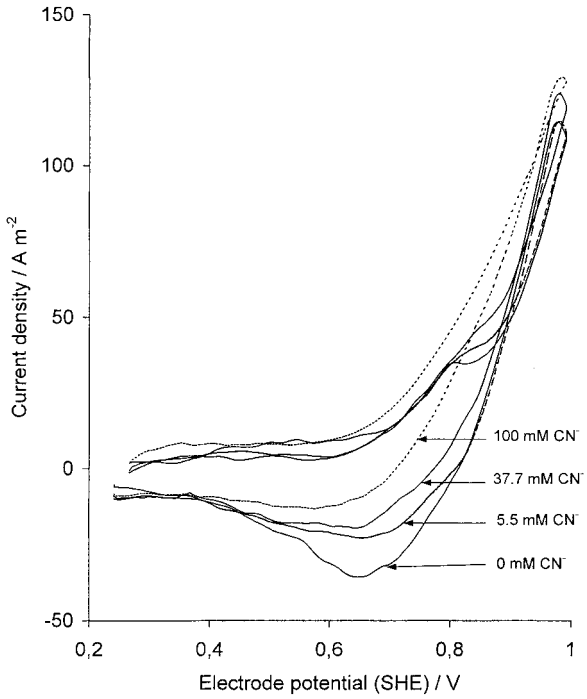

Fig. 2. Cyclic voltammograms of a Ti/Co_3O_4 electrode in 0.1 M NaOH. Cyanide concentration as indicated on the graph and potential scan rate of 20 mV s^{-1}.

are probably already reduced by a direct oxidation of CN^- ions.

Controlled potential coulometric experiments in the potential range 0.4–1.1 V vs SHE, followed by cyanate and cobalt determination in electrolyte, confirm that the current at potential on the wave prior to the onset of oxygen evolution is not due to cobalt dissolution but rather to the oxidation of cyanide. In these experiments, however, the cyanide oxidation is only observed at potentials far higher ($E > 600$ mV vs SHE) than those predicted from theoretical value (1) and seems to coincide with that for the change of oxidation state (Co^{3+}/Co^{4+}) of the cobalt within the surface metal oxide.

This experimental observation suggests that the cyanide oxidation occurs indirectly by reduction of the higher metal oxide (Co^{4+}) into the lower metal oxide (Co^{3+}):

$$CN^- + 2\,CoO_2 + H_2O = CNO^- + 2\,CoOOH \qquad (5)$$

A similar mechanism is commonly accepted for the oxidation of cyanide at nickel anode [28]. Nevertheless, in contrast with nickel anodes, the anodic dissolution of cobalt oxide deposit does not occur during cyanide oxidation since no cobalt ions are found in solution.

This high activity of the cobalt spinel anode towards cyanide oxidation could be explained by the synergistic combination of the high potential of the redox couple Co^{3+}/Co^{4+} and the well known affinity between cyanide and cobalt.

This oxidation mechanism could also explain the high catalyst activity in liquid phase cyanide oxidation with the cobalt oxide system developed by Christoskova et al. [29, 30]. This cobalt oxide catalyst is prepared chemically by reaction of NaOH and NaOCl with a cobalt nitrate aqueous solution. Analysis of the solid phase shows that cobalt is mainly present in the highest oxidation state (+4) since its composition is approached by the formula $CoO_{1.78}0.4\ H_2O$. Their interesting results confirm the high catalytic activity of cobalt oxide in its higher oxidation state for the aqueous cyanide oxidation.

3.2. *Galvanostatic experiments*

Prior to cyanide oxidation experiments, the Ti/Co_3O_4 electrode was galvanostatically pretreated (100 A m^{-2}) in a 0.1 M NaOH electrolyte during two hours. After this pretreatment, sodium cyanide concentrated solution was added to the solution for starting the cyanide electrooxidation. The resulting electrolyte had the following typical composition: 0.01 M NaCN and 0.1 M NaOH and was electrolysed at ambient temperature in an undivided flow cell. According to Figure 2, the current density at 780 mV vs SHE for a cyanide concentration in the range 5.5 to 37.7 mM is about 40 A m^{-2}. Turbulent conditions by a rapid pumping and by the use of turbulent promoters would typically increase this value by a factor of 2. For these reasons, galvanostatic experiments were done at a current density of 100 A m^{-2} to operate the reaction under mass transport control.

During depletion experiments, the electrolyte was periodically analysed for cyanide and cobalt concentration and the anodic potential was recorded.

Figure 3 reports experimental values of cyanide, cyanate concentrations, cell and anodic potentials against time.

When no cyanide ions are present, the anodic potential has a constant value of about 0.78 V vs SHE. As

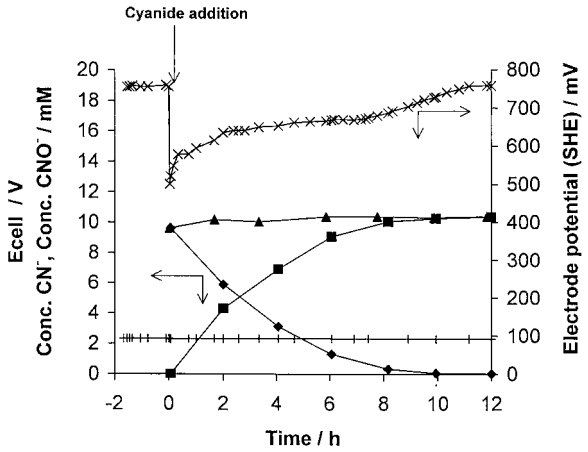

Fig. 3. Anodic potential (×), cell potential (+), cyanide (◆), cyanate (■) and nitrogen contents (▲, $[CN^-]$ + $[CNO^-]$-) as a function of time of cyanide electrooxidation. Operating conditions: electrolyte is 10 mM sodium cyanide in 0.1 M sodium hydroxide. Ti/Co_3O_4 anode, current density 100 A m^{-2}, treated volume 500 ml, linear flow velocity 2.5 cm s^{-1}.

soon as sodium cyanide is added to the alkaline solution, the anodic potential drops to 0.58 V vs SHE. Values obtained here confirm those observed on previous voltammograms, as the initial cyanide oxidation anodic potential coincides with the beginning of the anodic wave. As cyanide is progressively oxidized, the anodic potential rises to the characteristic value of the oxygen onset. At all times, the cobalt ion concentration is lower than 0.05 mg l^{-1}. It is also observed that the nitrogen mass balance ($[CN^-]$ + $[CNO^-]$) is satisfied during the course of cyanide electrooxidation. This means that Reaction 1 reflects the cyanide oxidation reaction and that cyanate ions are not further oxidized.

A comparison of cyanide oxidation efficiency was done for two other anodic materials, following the same modus operandi. Figure 4(a) shows these results and indicates that, despite its well known lower oxygen overpotential, the Co_3O_4 coated anode gives better results in comparison with graphite or DSA–O_2 anodes.

The decays also appear to be exponential with time and this could be confirmed by plotting $\ln[C_{(t)}/C_{(0)}]$ as a function of time, see Figure 4(b). This demonstrates that the cyanide oxidation is mass transport controlled in this concentration range. In fact, the expectation of linearity for $\ln[C_{(t)}/C_{(0)}]$ against time was confirmed, especially for the Co_3O_4 anode, only for the final portion of the curve. In this case, slopes from straight lines give an indication of the cell performance.

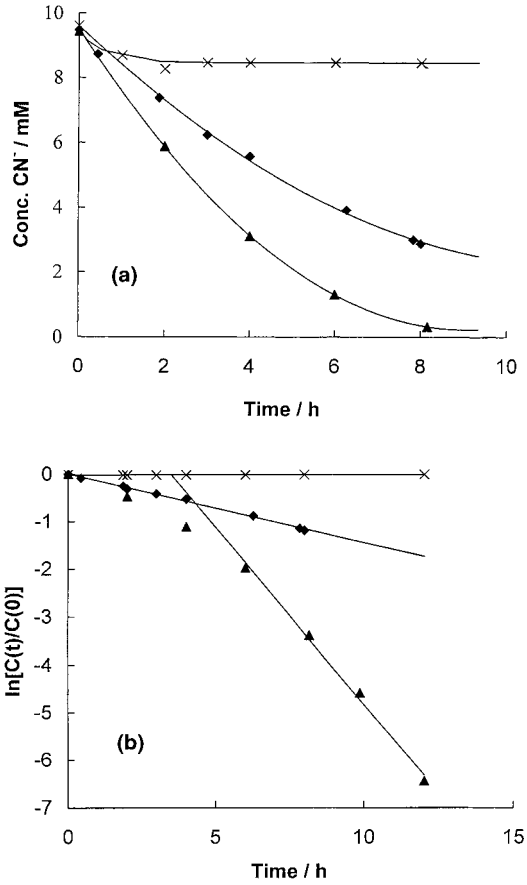

Fig. 4. (a) Cyanide concentration as a function of time for the three following anodic materials: DSA–O_2 (×), Graphite (◆), Ti/Co_3O_4 (▲). Operating conditions: electrolyte is 10 mM NaCN in 0.1 M NaOH, current density 100 A m^{-2}, linear flow velocity 2.5 cm s^{-1}. (b) Plots of $\ln[C(t)/C(0)]$ against time for the same data.

According to the model concentration-time relationships in recirculating electrochemical reactor systems proposed by Walker and Wragg [31], the slope is approximated by the following relation:

$$S = -\left[\frac{1 - \exp(-k_L A/Q)}{\tau}\right] \quad (6)$$

where Q is the electrolyte flow rate, A the anodic surface area, k_L the mass transfer coefficient and τ the residence time in the reservoir.

Table 1 shows values of k_L and faradic yields after 8 h treatment as a function of anode materials.

From these values it is clear that Ti/Co_3O_4 anodes are more effective than graphite. After 8 h, however, current efficiencies for Co_3O_4, graphite and DSA–O_2 anode are no higher than respectively 29.5%, 21.9% and 3.2%. These relatively low values may be explained by the fact that, due to the low cyanide concentration, in the potential where cyanide reacts, the concurrent oxidation of hydroxide to oxygen is the major source of current inefficiency.

It should also be pointed out that the values of k_L calculated here are higher than the usual values which are in the region of 10^{-5} m s^{-1} [32]. It is well known that turbulence promoters increase k_L by a factor of 2 to 3 [33–35]. The oxygen bubbles evolving in the loss reaction are also probably responsible for the mass transport enhancement. Finally, the rough deposit of cobalt spinel on Ti plate may explain the difference between the two values of k_L.

Even with a too high current density, the average current efficiency and d.c. power consumption for reducing the cyanide concentration from 1×10^{-2} to 2×10^{-4} M on a Ti/Co_3O_4 anode reach about 28.5% and 18 kWh kg^{-1} CN^- oxidized, respectively. It is noteworthy that this latter energy consumption is lower than those published elsewhere [14–16, 19, 36].

Hence, Spinel cobalt oxide appears to be a suitable anode material for the oxidation of cyanide taking into account its electrocatalytic properties, its electrochemical stability and its durability. As an example, Ti/Co_3O_4

Table 1. Effect of the anode material on the oxidation of cyanide from alkaline solution. Operating conditions: electrolyte is 10 mM NaCN in 0.1 M NaOH, current density 100 A m^{-2}, linear flow velocity 2.5 cm s^{-1}

Anode material	k_L /m s^{-1}	Faradic yield /%
DSA–O_2	–*	3.2
Graphite	2.04×10^{-5}	21.9
Ti/Co_3O_4	10.43×10^{-5}	29.5

* Not measured

electrodes were used for more than 200 h in galvanostatic experiments without significant surface degradation. In all cases, the cobalt concentration in the electrolyte never exceeded 0.05 mg dm^{-3}.

4. Conclusion

Cobalt oxide deposited on Ti substrate by thermal decomposition shows outstanding properties for the electrooxidation of cyanide ions. The efficiency and durability of these Ti/Co_3O_4 anodes result from three characteristics:

(i) The high electroactivity of cobalt oxide is mainly due to the equilibrium potential of Co^{3+}/Co^{4+} located in the potential range of cyanide oxidation.
(ii) Cyanide ions can be easily adsorbed on cobalt oxide due to the high affinity between cobalt and cyanide.
(iii) The Co^{3+} and Co^{4+} species are virtually insoluble so that the durability of such oxide layers is very high.

The specific energy consumption for the reduction of the cyanide concentration from 1×10^{-2} to 2×10^{-4} M (98% elimination of cyanide) on Ti/Co_3O_4 reaches about 18 kWh kg^{-1} CN^- oxidized. Furthermore, this d.c. power consumption could be reduced by optimizing the electrolysis conditions such as pH, current control and cell design. It should also be noted that the spinel coating could be used for many batches or long-term electrolyses without apparent loss of activity or physical/chemical damage.

However, as cyanide ion is highly toxic, its limiting concentration in effluent should be lowered to as low as 1 mg l^{-1}. In this context, a special electrolysis cell must be used in order to increase the mass transfer, thereby improving the current efficiency at very low cyanide concentrations. To resolve this mass transfer limitation, the use of three-dimensional electrodes should be investigated. For this reason, further experiments have been carried out with porous electrodes coated with cobalt oxide. These further results will be presented in a latter paper.

References

1. L. Hartinger, 'Handbook of Effluent Treatment and Recycling for the Metal Finishing', 2nd edn, Finishing Publications Ltd, Stevenage, (1994).
2. J. Marsden and I. House, 'The Chemistry of Gold Extraction', Ellis Horwood, Chichester, (1992).
3. C.A. Young, S.P. Cashin and F.E. Diebold, *in* M. Misra (Ed), 'Separation Processes Heavy Metals, Ions and Minerals', TMS, Warrendale, PA, (1995), pp. 61–80.
4. C.A. Young, *in* B. Mishra (Ed), 'EPD congress 1998', TMS, Warrendale, PA, (1998), pp. 877–886.
5. B.R. Kim, D.H. Podsiadlik, E.M. Kalis, J.L. Hartlund and W.A. Gaines, *J. Environ. Eng.* **24** (1998) 1108.
6. J.B. Mosher and L. Figueroa, *Miner. Eng.* **9** (1996) 573.
7. J. Whitlock, *J. Metals* **41** (1989) 161.
8. V. Augugliaro, V. Laddo, G. Marci, L. Palmisano and M.J. Lopez-Munoz, *J. Catal.* **166** (1997) 272.
9. V. Augugliaro, J. Blanco Galvez, J. Caceres Vasquez, E. Garcia Lopez, V. Loddo, M.J. Lopez Munoz, S. Malato Rodriguez, G. Marci, L. Palmisano, M. Schiavello and J. Soria Ruiz, *Catal. Today* **54** (1999) 245.
10. H. Tamura, T. Arikado, H. Yoneyama and Y. Matsuda, *Electrochim. Acta* **19** (1974) 273.
11. J.K. Easton, *Plating* **53** (1966) 1340.
12. J.M. Connard and G.P. Beardsley, *Met. Finish.* **59** (1961) 54.
13. T. Arikado, I. Iwakura, H. Yoneyama and Y. Matsuda, *Electrochim. Acta* **21** (1976) 1021.
14. T.C.Wen, *Plat. Surf. Finish.* **77 (**1990) 54.
15. S. Christoskova and S. Maric, *Env. Prot. Eng.* **17** (1991) 93.
16. Z. Parisheva and E. Kanova, *Galvanotechnik* **89** (1998) 1265.
17. A. Perret, W. Haenni, N. Skinner, X-M. Tang, D. Gandini, C. Comninellis, B. Correa and G. Foti, *Diamond Relat. Mater.* **8** (1999) 820.
18. F. Hine, M. Yasuda, T. Ida and Y. Ogata, *Electrochim. Acta* **31** (1986) 1389.
19. C.S. Fugivara, P.T.A. Sumodjo, A.A. Cardoso and A.V. Benedetti, *Analyst* **121** (1996) 541.
20. B. Wels and D.C. Johnson, *J. Electrochem. Soc.* **137** (1990) 2785.
21. J. Feng and D.C. Johnson, *J. Electrochem. Soc.* **134** (1987) 507.
22. H. Klenk, A. Griffiths, K. Huthmacher, H. Itzel, H. Knorre, C. Voigt and O. Weiberg, *in* 'Ullmann's Encyclopedia of Industrial Chemistry', vol. A8, 5th edn, VCH, Weinheim, (1987), pp. 159–190.
23. P. Cox and D. Pletcher, *J. Appl. Electrochem.* **20** (1990) 549.
24. P. Cox and D. Pletcher, *J. Appl. Electrochem.* **21** (1991) 11.
25. C. Henry and J-C. Boeglin, *Revue du Cebedeau* **331–332** (1971) 282.
26. R. Garavaglia, C.M. Mari and S. Trasatti, *Surf. Technol.* **23** (1983) 197.
27. R. Boggio, A. Carugati and S. Trasatti, *J. Appl. Electrochem.* **17** (1987) 828.
28. G.H. Kelsall, S. Savage and D. Brandt, *J. Electrochem. Soc.* **138** (1991) 117.
29. S. Christoskova, M. Stojanova and D. Mehandzhiev, *Galvanotechnik* **87** (1996) 4124.
30. S. Christoskova, M. Stojanova, M. Georgieva and D. Mehandzhiev, *Mat. Chem. Phys.* **60** (1999) 39.
31. A.T.S. Walker and A.A. Wragg, *Electrochim. Acta* **22** (1977) 1129.
32. D. Pletcher, *in* J.D. Genders and N.L. Weinberg (Eds), 'Electrochemistry for a Cleaner Environment', The Electrosynthesis Company, New York, (1992), pp. 11–51.
33. L. Lipp and D. Pletcher, *Electrochim. Acta* **42** (1997) 1101.
34. L. Carlsson, B. Sandegren and D. Simonsson, *J. Electrochem. Soc.* **130** (1983) 342.
35. T.R. Ralph, M.L. Hitchman, J.P. Millington and F.C. Walsh, *Electrochim. Acta* **41** (1996) 591.
36. A.T. Kuhn and K. Biddle, *Oberflache-Surface* **18** (1977) 182.